Progress In Electromagnetics Research M, Vol. 12, 115–130, 2010

ANALYSIS OF SELF-COLLIMATION BASED CAVITY RESONATOR FORMED BY PHOTONIC CRYSTAL

N. Yogesh and V. Subramanian

Microwave Laboratory, Department of Physics
Indian Institute of Technology Madras
Chennai-600036, India

Abstract—The self-collimation effect in photonic crystal is used for the realization of open cavity resonator formed by photonic prisms in a four-port arrangement. The confinement, field enhancement and energy storage capabilities of the proposed cavity are explored in this paper. The effect of dielectric losses included in the system and role of the position of line source in the confinement effect of the cavity are brought out. Decay of short Gaussian pulse placed inside the cavity is analyzed through finite-difference time-domain studies. Due to the high confinement and divergence less beam propagation, utility of the proposed cavity for rotational gyroscope application is also revealed.

1. INTRODUCTION

The electromagnetic wave propagation in periodic structures (also called photonic crystals-PCs) sees two extremes: 1) forbiddance [1] and 2) anomalous dispersion, which are effectively employed for the development of guided, refracted and radiated systems in microwave and optical length scales. In particular, the two main branches of the anomalous dispersion in photonic crystals consisting of flat dispersion regime (results in self-collimation) [2] and convex/concave shaped dispersion regime (results in all angle negative refraction) [3] offer novel photonic elements like sharp bends [4], beam splitters [5] and sub-wavelength imaging lens [6], open cavities [7, 8] respectively.

Among these, PCs are given much attention for the confinement of electromagnetic waves and localization of photons in the form of realization of cavity resonating structures [7–9]. In principle, the realization of cavity resonating structures can either be based on band

Corresponding author: V. Subramanian (manianvs@iitm.ac.in).

gap effect, in which the creation of defect sites in the PC leads to formation of cavity [9] or be based on anomalous dispersion in PCs such as self-collimation and negative refractive effect. Based on negative refraction, open cavity was proposed [7] and wave confinement effect was demonstrated numerically [8]. However, the cavity based on negative refraction has possible demerits such as the effect of truncation and termination of PC layers and dielectric losses in the system, which eventually results in degradation of confinement. As an alternative one can also relay on self-collimation in PC for wave confinement. In 2008, Shen et al. addressed the self-collimation based cavity in a channel-less PC for effective waveguide mechanism [10].

The aim and motivation of the present work is to reveal the characteristics of self-collimation based cavity resonator such as its confinement, field enhancement and energy storage abilities. With respect to the conventional reflection based resonator, the confinement ability of the proposed cavity is mainly due to the flat dispersion regime of the PC, which leads to divergence less beam propagation and confinement of fields along its collimated path. Field enhancement results from a constructive interference of field components emitted by the line source placed inside the cavity and the minimum radiated power away from the structure reveals the energy storage aspect.

Photonic prism made of periodic arrangement of dielectric rods having relative permittivity of $\varepsilon_r = 5.5$ (for example ordinary glass rods) in an air medium arranged in four-port is considered for the characterization studies of the open cavity. The analysis includes the phase matching condition, cavity lifetime, quality factor (Q) calculations through finite-element (FEM) [11] and finite-difference time-domain methodologies (FDTD) [12]. The confinement effect is demonstrated with the inclusion of dielectric losses and the dependence of position of line source in Q factor of the proposed cavity is brought out. The decay of short Gaussian pulse placed inside the cavity is analyzed through FDTD method, which emphasizes this proposed cavity as an effective energy storage element. The question of utilizing this cavity for rotational gyroscope application is also revealed in this work.

2. BAND STRUCTURE AND SELF-COLLIMATION FOR FORMATION OF OPEN CAVITY

The PC consists of square lattice based periodic arrangement of dielectric rods with relative permittivity of $\varepsilon_r = 5.5$ and normalized radius of $r = 0.41667a$ ('a' is the lattice period) in an air background. For microwave applications 'a' is chosen to be 1.2 cm as the basic

length-scale, which leads to the diameter of the rod to 1 cm. For the calculation of photonic band structure, the electromagnetic solver MPB [13] is used, which treats the Maxwell's wave equation as a Hermitian eigenvalue problem with the plane wave basis. The work is carried out with transverse magnetic polarization (TM), where magnetic field is perpendicular to the axis of the dielectric cylinders. It is to be noted that the definition of polarization is given with respect to the axis of the cylinders rather than the direction of propagation.

Figures 1(a) and 1(b) show the band diagram and equifrequency surface (EFS) of the square lattice of dielectric rods in an air background respectively. The flat region of the EFS plot in the repeated zone scheme given in Figure 1(b) corresponds to the normalized frequency of $\omega = 0.27523(\frac{2\pi c}{a})$. In an effective homogenous medium, the normal drawn to the EFS can be regarded as the direction of propagated signal. Hence an electromagnetic wave of frequency around $\omega = 0.28(\frac{2\pi c}{a})$ is incident towards the ΓM symmetry direction in the PC results in unaltered beam propagation with the maintenance of beam width (self-collimation effect). This self-collimating frequency region is entirely lies within the first band as shown in the Figure 1(a), which asserts the condition of single beam propagation given in Ref. [3] by $\omega \leq 0.5(\frac{2\pi c}{a_s})$ ('a_s' is the surface period of the PC).

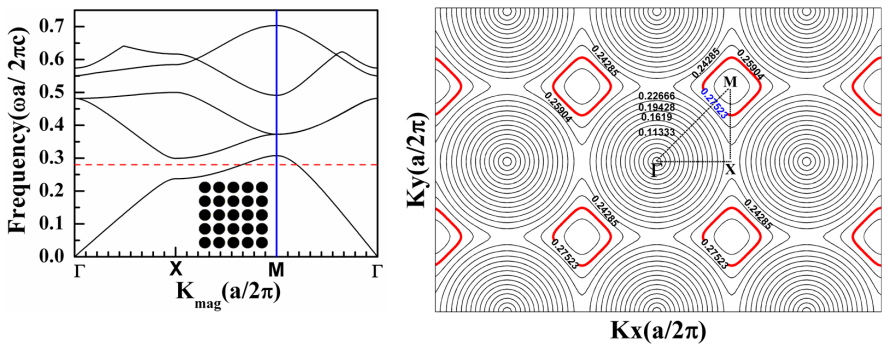

(a) (b)

Figure 1. (a) The TM mode band structure of square lattice PC consists of rods with the relative permittivity (ε_r) of 5.5 in an air. The inset shows the PC structure with the normalized radius of $0.41667a$. The operational frequency is indicated with the dotted line. (b) The equifrequency surface plot of the first TM band of the square lattice PC. The flat line corresponds to normalized frequency (ω) of $0.27523(2\pi c/a)$ is indicated with the bold line in the plot.

For this corresponding frequency, the total reflection of self-collimated beams at the truncated surface of the photonic prism is given through finite-element methodology [11]. The prism arrangement consists of 14 layers of dielectric rods in the base and length sides. Since the self-collimation is in the vicinity of ΓM symmetry direction, PC prism layers are arranged towards ΓM direction, which has a surface period of $a_s = \sqrt{2}a$. To have a normal incidence, the line source is placed parallel to the base of the photonic prism. Studying this open system, low reflecting boundary condition (similar to perfectly matched layers (PML) [12]) is employed around the computational domain. The intensity profile given in Figure 2(a) corresponds to the frequency of 7.000789 GHz confirms the self-collimation effect by the PC. Including the shift at the truncated surface of the PC prism (Goos-Hänchen (GH) shift), the computed total reflection is above 96% for TM polarized wave, which indicates that the PC prism acts as a good mirror and it will be the basic element for realization of the cavity. Figure 2(b) shows the geometry of the cavity resonator studied in this work, which is formed by PC prisms arranged in four-port. The prisms are separated with the spacing of d_1 and d_2 in the horizontal and vertical dimension of the cavity respectively and characterization is done within the self-collimating regime in the range of 6.98 GHz to 7.02 GHz.

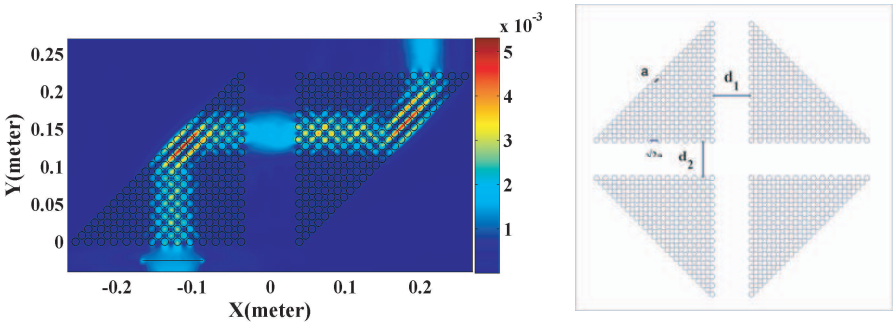

(a) (b)

Figure 2. (a) The intensity plot of total reflection of self-collimated beam at the frequency of 7.000789 GHz for a line source kept in parallel with the base of the PC prism at $(-0.15\,\text{m}, -0.025\,\text{m})$ [this is equivalent to $(-12.5a, -2.0833a)$]. 'a' is the lattice constant taken to be 1.2 cm. (b) The model of the cavity resonator.

3. CHARACTERIZATION

3.1. Phase Matching Condition

The resonance behavior of the proposed cavity mainly depends on the cavity spacing values (d_1 and d_2), and by tuning them the desired single frequency mode within self-collimated regime can be selected. The condition on the cavity resonance is given by equating the round trip phase to an integral multiple of 2π, and it is written as

$$2Kd_1 + 2Kd_2 + K_{\text{effective}}l = 2\pi p \tag{1}$$

where p is an integer, and l is the distance traveled by the wave within four prisms. d_1 and d_2 are the cavity spacing in the horizontal and vertical dimensions respectively. $K = \frac{n\omega}{c}$ is the propagation constant of the wave in the air medium ($n = 1$), and $K_{\text{effective}} = \frac{n_{\text{effective}}\omega}{c}$ is the propagation constant of the wave in the prism medium, where ω is the angular frequency of electromagnetic wave, and $n_{\text{effective}}$ is effective refractive index of the PC medium. To evaluate the effective index of the composite PC, vector nature of the electromagnetic waves is considered through Maxwell-Garnet relation [14], which is expressed as

$$\frac{1}{n_{\text{effective}}} = \sqrt{\frac{1}{\varepsilon_r}f + (1-f)} \tag{2}$$

The effective index given in Equation (2) corresponds to the periodic arrangement of dielectric cylinders ($\varepsilon_r = 5.5$) in an air background. f is the filling ratio (the volume fraction occupied by the dielectric cylinders in an air background). For a normalized radius of $r = 0.41667a$, in a square lattice basis, the filling factor is 0.5454. Substituting the value of ε_r and f in Equation (2), the evaluated effective index is $n_{\text{effective}} = 1.344$. The expression for the resonance frequency from Equation (1) can be written as

$$f_{\text{resonance}} = \frac{cp}{(2d_1 + 2d_2 + n_{\text{effective}}l)} \tag{3}$$

where $\text{f}_{\text{resonance}}$ is the self-collimating frequency. It is important to obtain the precise value of GH shift, to evaluate the distance l traveled by the wave in four prisms. If one assumes the geometrical length of the four prisms as the distance traveled by the wave, then l is to be $4\times13\sqrt{2}a$. Substituting the value of l in Equation (3) for a typical self-collimating frequency $f = 7\,\text{GHz}$, cavity spacing values of $d_1 = 6.473a$ and $d_2 = 5.581a$ with the $n_{\text{effective}}$ value of 1.344, the value of p is evaluated to be 34.

As an alternative to count the number of full wavelength variation within the prisms, the resonance condition can be easily verified against

single frequency by examining the mode variation within the cavity spacing itself. In order to verify the resonance condition given in Equation (1), the cavity spacing d_2 is fixed to be 1.75λ, and the distance of d_1 is varied as 2λ, 2.5λ, and 3λ where λ is the free space wavelength. For a single frequency operation, λ is taken to be 4.28523 cm, which lies in the self-collimating regime. Plugging these d_1 and d_2 values in Equation (1), the resonance condition reads as

$$\begin{aligned} 7.5\lambda + n_{\text{effective}} l &= p_1 \lambda \\ 8.5\lambda + n_{\text{effective}} l &= p_2 \lambda \\ 9.5\lambda + n_{\text{effective}} l &= p_3 \lambda \end{aligned} \tag{4}$$

where p_1, p_2 and p_3 are integral numbers of full wavelength variations corresponding to the cavity spacing distance (d_1) 2λ, 2.5λ and 3λ respectively.

It is obvious from the set of equations given in Equation (4) that the number of full wavelength variations in the cavity is varied in step one, with respect to 0.5λ variation in spacing d_1 and the field pattern corresponding to d_1 for 2λ, 2.5λ and 3λ shown in Figures 3(a)–3(c) respectively, which confirms the above mentioned resonance condition (one can count the number of wavelength variations in the cavity spacing gap).

It is also possible to demonstrate the condition of destructive interference for the proposed cavity. There are two possible mechanisms to do this. The first one involves the movement of the source's position. By moving the position of the source, one can create the path difference between the clockwise (CW) and counterclockwise (CCW) propagating beams inside the cavity. In such a case, whenever the path difference (S) between the clockwise (CW) and counterclockwise (CCW) propagating beams is an odd integral multiples of half-wavelength ($\frac{\lambda}{2}, \frac{3\lambda}{2}, \frac{5\lambda}{2}, \ldots$), and the interference is strictly destructive (the corresponding phase difference would be $\pi, 3\pi, 5\pi, \ldots$), and it can be expressed as

$$S = (2n-1)\,\frac{\lambda}{2}, \quad n = 1, 2, 3, \ldots. \tag{5}$$

Figure 3(d) reveals the case of destructive interference as per Equation (5). With respect to Figure 3(a), the source is moved up by $\lambda/4$ (so that a path difference of $\lambda/2$ is achieved between the CW and CCW propagating beams) in Figure 3(d). This manifests a phase difference of π between the CW and CCW beams, so that the waves will reinforce destructively.

As a second mechanism, based on Equation (5), the destructive interference can also be explained in terms of cavity spacing values d_1

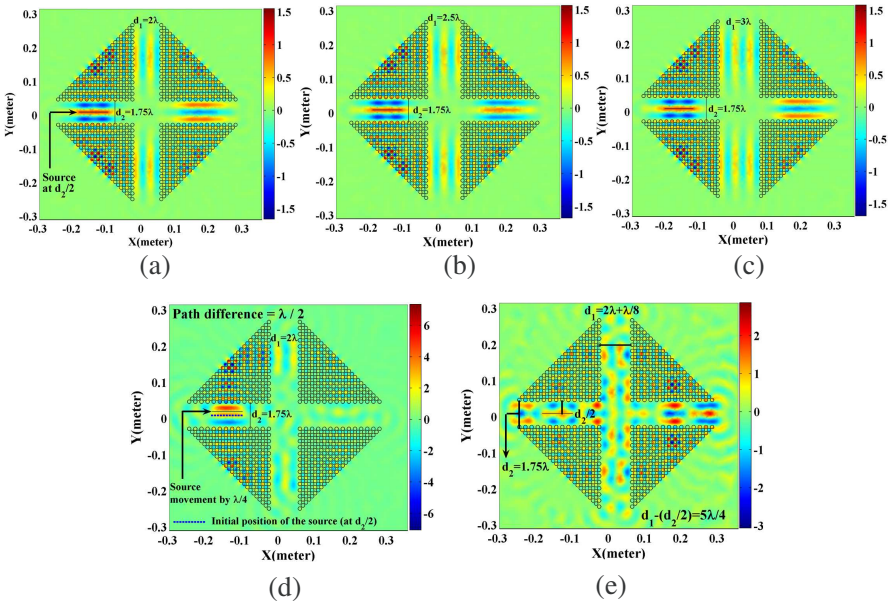

Figure 3. For a fixed cavity spacing d_2 of 1.75 λ, (a), (b), and (c) show the mode variations correspond to the cavity spacing d_1 for 2λ, 2.5λ and 3λ respectively. (d) The case of the destructive interference with respect to the source movement. (e) The case of destructive interference with respect to the cavity spacing values. Here λ is taken to be 4.28523 cm, which lies in the self-collimating regime.

and d_2. Whenever, the difference of $d_1 - \frac{d_2}{2}$ is an odd integral multiple of $\lambda/4$, the interference is destructive, and it can be expressed as

$$d_1 - \frac{d_2}{2} = (2n-1)\frac{\lambda}{4}, \quad n = 1, 2, 3, \ldots \tag{6}$$

where d_1 is the horizontal cavity spacing, and $d_2/2$ is the distance between the source and incident photonic prism (indicated in Figure 3(e)). Figure 3(e) verifies the condition of destructive interference as per Equation (6) [With respect to Figure 3(a), in Figure 3(e), the distance d_1 is increased by $\lambda/8$, so that a difference in $d_1 - \frac{d_2}{2}$ of $5\lambda/4$ is arrived (which leads to the destructive interference)]. It should be noted that the constructive interference given in Equation (4) and the destructive interference given in Equation (6) are obtained based on the fixed source's position (i.e., the source is always at the central part of the photonic prism and placed at $d_2/2$ along the y axis).

3.2. The Wave Confinement Effect

To probe the confinement of field components inside the cavity, lifetime calculations are performed using FEM corresponding to the cavity spacing values of $d_1 = 6.473a$ and $d_2 = 5.581a$. Since the lifetime simply compares the energy stored in the cavity to the averaged power radiated per cycle, the normalized lifetime of the cavity is expressed as [8],

$$\frac{T_{\text{structure}}}{T_{\text{air}}} = \frac{W_{\text{structure}} P_{\text{air}}}{W_{\text{air}} P_{\text{structure}}} \tag{7}$$

where $T_{structure}$ and T_{air} represent the lifetime values in the photonic structure and air respectively. $W_{\text{structure}}$ is the time average, total energy density stored in the cavity and $P_{\text{structure}}$ is the norm of time average power flow, radiated outside the cavity. The expressions for total energy density and the power flow are in-built functions in all electromagnetic solvers like FEMLAB [11], MPB [13] and MEEP [16]. The calculations of $W_{\text{structure}}$ and $P_{\text{structure}}$ involve the spatial integration of respective expressions over the defined area in the following manner; 1) To calculate the $W_{\text{structure}}$, the area enclosed by the perimeter of the cavity is taken and the spatial integration is performed over that area; 2) To calculate the $P_{\text{structure}}$, the area bounded between the computational domain and the perimeter of the cavity is taken and the integration is performed over that area; 3) To uniquely represent the confinement through this calculation, the values are normalized with respect to the integrated values (W_{air} and P_{air}) corresponding to the empty space (without the PC structure). This is to eliminate the discrepancies involved in the computational domain size and the area selection. So that, even if one changes the domain size, the confinement is always corresponds to specific frequency regardless of the normalized values.

Figure 4(a) shows the variation of normalized cavity lifetime with respect to change in the frequency within self-collimating regime, corresponding to the line source positioned at $(-8.3375a, -2.0833a)$. For a specific length scale of $a = 1.2\,\text{cm}$, the position of line source is at $(-0.10005\,\text{m}, -0.025\,\text{m})$ inside the cavity (One can see the position of line source from Figure 4(b)). The frequency 6.99407 GHz has the normalized lifetime value of 1150 ($T_{\text{structure}}/T_{\text{air}}$) and the corresponding field pattern given in Figure 4(b) reveals the confinement of fields along the collimated path.

This confinement effect of the proposed cavity is further verified by introducing the dielectric losses in the system. Figure 4(a) shows the variation of normalized cavity lifetime against the variation in the dielectric losses ranging from $\varepsilon_r'' = 0.005$ to $\varepsilon_r'' = 0.025$ (ε_r'' be the

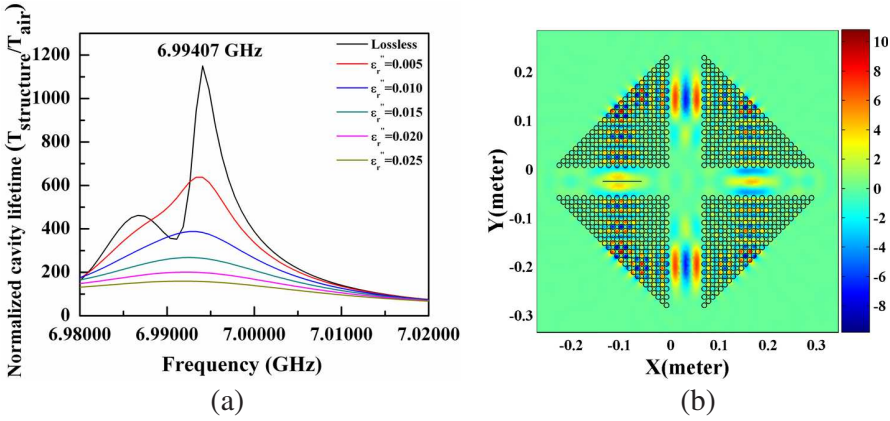

Figure 4. (a) The plot of normalized cavity lifetime for the self-collimating frequencies with inclusion of dielectric losses in the system. (b) The E_z component at 6.99407 GHz reveals the confinement for the line source positioned at $(-0.10005\,\text{m}, -0.025\,\text{m})$ [equivalent to $(-8.3375a, -2.0833a)$].

imaginary part of the complex relative dielectric permittivity) and the high value of normalized lifetime reveals the existence of confinement even in the presence of dielectric losses.

3.3. Quality Factor and Role of Line Source's Position

The field enhancement and energy storage ability of the cavity can be explored through quality factor (Q) computations. In this work, the two kinds of Q factor computations are carried out: 1) plane wave based calculations using FEM and 2) behavior of short Gaussian pulse placed inside the cavity through FDTD method.

To proceed with plane wave based calculations using FEM, the computational domain consists of the cavity is discretized with finer meshes and spectral response of the cavity is monitored for a line source placed inside the cavity. The position of line source and the computational domain is being same as that shown in Figure 4(b). The intensity (the norm of time average, power flow) of the running wave is monitored by the line detector, which is placed in such a way to cover the bright spot of the cavity mode. For example, referring with Figure 4(b) the line detector is placed anywhere within the cavity spacing either in d_1 or d_2, in the direction of propagation of fields.

For self-collimating frequency regime, the spectral profile is plotted in Figure 5(a). According to the intensity measurement, the

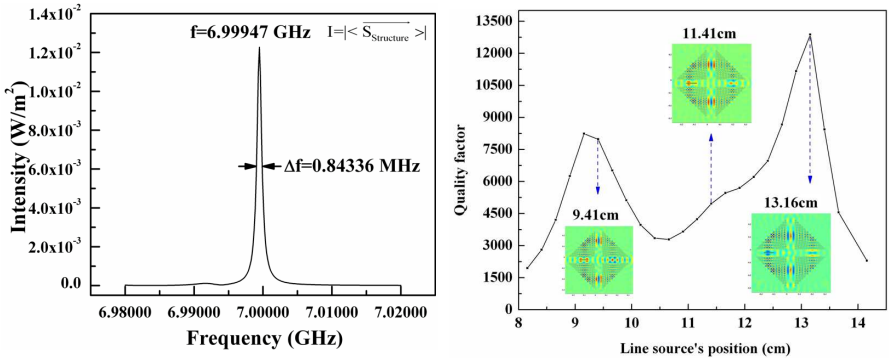

Figure 5. (a) The plot of intensity of running wave inside the cavity against self-collimating frequency regime. (b) The role of line source's position on the Q factor of the cavity. The E_z field patterns at different line source's positions are given in the inset.

expression for the Q factor is given by,

$$Q = \frac{f}{\Delta f} \tag{8}$$

where f is the resonance frequency and Δf is the full width at half maximum (FWHM) of the spectral response. At frequency 6.99947 GHz, the computed FWHM is $\Delta f = 0.84336$ MHz and it leads to the Q factor value of 8300. Such a high value uniquely represents the field enhancement (height of the spectral peak) and energy storage ability (further revealed in next section) of the proposed cavity for plane waves. It should be noted that the Q factor computation is 2D dimensional, where the third dimension (height of the rod is taken to be infinity) is not considered. In such a case, the out of plane radiation losses due to finite height of dielectric pillars degrades the high Q value. However one might reduce the out of plane radiation losses due to finite height, by keeping the ratio of rod height to the applied wave length to be very high [15].

Apart from the Q factor calculation to the fixed position of the line source, significant variation in Q factor is found with respect to change in the horizontal position of the line source, which is revealed in Figure 5(b). The E_z field patterns given in the inset of Figure 5(b) corresponds to line source placed at 9.41 cm, 11.41 cm and 13.16 cm inside the cavity. Here the distance of the line source is measured (referring with Figure 4(b)) with respect to base corner of the first photonic prism. The distance traveled within the effective dielectric

medium and the air-gap (as well as one geometrical round trip distance) is same irrespective of the position of line source. The Q factor variation within the region between 10.4 cm to 13 cm corresponds to the line source's position kept at the central portion of the photonic prism. As expected near the edges of the photonic prism the Q factor is low due to scattering effect. At the same time, it is important to include the factors such as Goos-Hänchen shift and radiation losses for one complete round trip to account for the nature of Q factor variation inside the cavity.

4. TIME DOMAIN STUDIES ON FIELD COMPONENTS INSIDE THE CAVITY

The behaviour of short Gaussian pulse placed inside the cavity is analyzed through FDTD based electromagnetic solver MEEP [16]. The geometry of the resonator is taken in the computational domain of $65a \times 65a$ around that perfectly matched layers of thickness $2a$ are employed, where 'a' is the fundamental length-scale. Gaussian beam of size $8a$ is centered on normalized frequency $f = 0.2784(\frac{c}{a})$ with the frequency width $\Delta f = \frac{1}{\Delta t} = 0.01(\frac{c}{a})$ is launched inside the cavity resonator at $(-11.4789a, -2.79044a)$. [This position is measured with respect to the center of the cavity resonator. In FDTD studies, center of the cavity resonator and center of the computational domain are same]. To have TM polarized beam, E_z current component is specified in the source definition.

4.1. Pulse Decay

Decay of such a short Gaussian pulse inside the cavity is described by monitoring the power flux of the field components and hence flux detector of size $8a$ is defined in the source region itself. The source is placed at $d_2/2$ of the left port of the cavity and after complete decay of the pulse the same region is considered for detecting the power fluxes.

In order to ensure the convergence of Fourier transform of field components, the following conditions are rigorously followed: 1) the calculations are kept running with an additional time units even after the source is turned off and 2) the intensity of running wave is monitored only when $|E_z|^2$ value of the pulse is decayed into $\frac{1}{1000}$ of its peak value. These conditions are facilitated via an in-built function in the solver.

In an air regime, with out the cavity resonator, the $|E_z|^2$ value of the Gaussian pulse will take 1000 time units to decay to $\frac{1}{1000}$ of its peak value. For the normalized frequency of $f = 0.2784\left(\frac{c}{a}\right)$, 1000 time

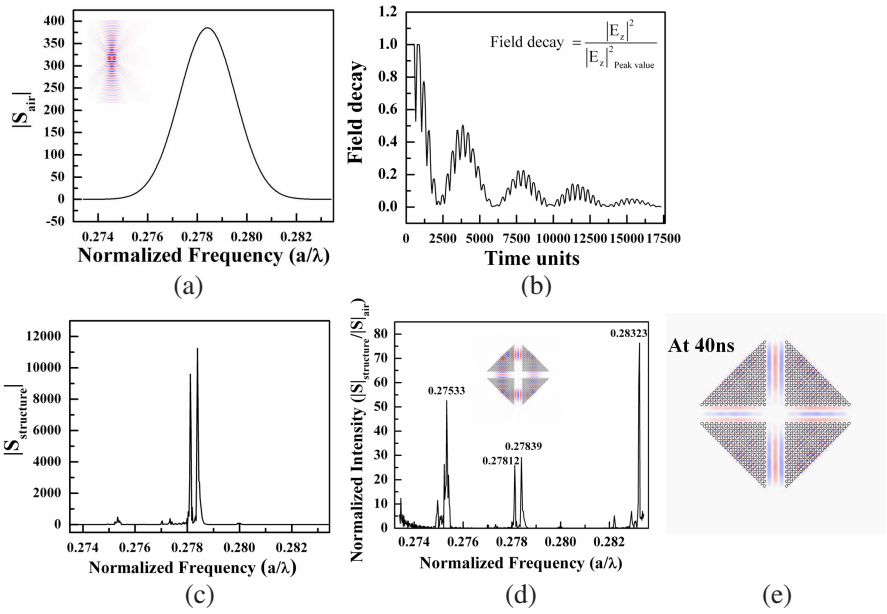

Figure 6. (a) The intensity plot recorded at 1000 time units corresponds to Gaussian pulse of size $8a$ with the normalized frequency (f) of $0.2784(c/a)$ and with pulse width (Δf) of $0.01(c/a)$. Inset shows the pulse propagation at 50 time units (2 ns). (b) The plot of field decay against time units shows the oscillation behaviour of field components inside the cavity. (c) The intensity spectrum of fields inside the cavity recorded after 17318 time units. (d) Normalized intensity spectrum of the cavity. In the inset, E_z component at 800 time units (32 ns) correspond to the normalized frequency (ω) of $0.27812(c/a)$ is given. (e) To show the confinement ability of the cavity, E_z component at 1000 time units (40 ns) corresponds to the frequency (ω) of $0.2784(c/a)$ is given.

units represent 278 periods of the pulse, which is equal to 39.94 ns for microwave length-scale of $a = 1.2$ cm. Figure 6(a) shows the intensity spectrum of the Gaussian pulse propagating in an air and an inset in the Figure 6(a) shows the E_z component of the field variation at 50 time units (2 ns).

As in the case of the cavity, the pulse will survive for a very long time of about 17318 time units due to strong resonance behavior and oscillation of field components inside the cavity is observed. This is revealed in Figure 6(b), which shows the plot of field decay (mentioned previously as the ratio of $|E_z|^2$ to its peak value) against

the time units. The complete decay of the pulse inside the cavity will take 4821 time periods and recording the intensity after this long time is given in Figure 6(c). Upon normalizing the intensity of the fields with and without the structure, the Q value of the cavity resonator can be terminated, in the normalized intensity spectrum shown in Figure 6(d). By measuring the FWHM of the spectral response in Figure 6(d) for the normalized frequencies of $0.27533(\frac{c}{a})$, $0.27812(\frac{c}{a})$, $0.27839(\frac{c}{a})$, $0.28323(\frac{c}{a})$ the obtained Q factor values are 5903, 5740, 4973, and 5777 respectively.

In order to emphasize the energy storage ability of the proposed cavity (the high Q value of the cavity), E_z field variation at 225.5 time periods (32 ns — the time at which field enhancement will be maximum due to reinforcement) is given in an inset of Figure 6(d) which corresponds to the normalized frequency of $f = 0.27812\left(\frac{c}{a}\right)$. Figure 6(e) gives the proof for the confinement effect of the cavity, which shows the E_z field variation at 1000 time units (40 ns). Mainly because, the same 1000 time units represent the time for complete decay of Gaussian pulse of normalized frequency $f = 0.2784\left(\frac{c}{a}\right)$ in an air medium.

4.2. Proposed Cavity as Rotational Gyroscope

As it is shown from FEM and FDTD results (Figures 3 and 7) that the modes supported by this cavity resonator are standing wave patterns. These standing wave patterns are formed by constructive interference between the clockwise (CW) and counter clockwise (CCW) propagating beams emitted by the line source placed inside the cavity. It is the key role for the realization of rotational gyroscopes in microwave/optical regime, which utilize the famous Sagnac effect [17] (the phase shift introduced between the CW and CCW beams upon rotation of the cavity with an angular velocity). By measuring change in the resonance frequency due to the phase shift upon rotation of the cavity, one can track the rotational speed accurately.

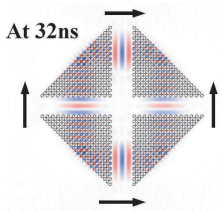

Figure 7. The visualization of the cavity for gyroscope application. E_z field component corresponds to the normalized frequency (f) of $0.2784(c/a)$.

Sunada et al. [18] reported Sagnac effect in resonant microcavities and they revealed that the change of standing wave resonance into a rotating wave, for a threshold value of rotational velocity of microcavity upon rotation. Similarly one can anticipate this proposed cavity for Sagnac ring and rotational gyroscope applications with the following advantages: 1) Though rotational gyroscopes are predicted, based on band gap effect in PC, the classical formulation of Sagnac effect cannot be applied directly [19]. This demands the design of dispersion based PC cavity so that one can apply the classical formulation directly, 2) conventional Sagnac ring suffers from divergence effect, whereas the proposed cavity is based on self-collimation effect results in divergence less beam propagation and this aspect of maintenance of beam width is expected for improving the accuracy of rotational frequency measurements (In particular, this is advantageous for realization of gyroscopes in microwave regime), 3) the minimum radiated power away from the structure (Referring with cavity lifetime) is appreciable for any rotational sensors, which are based on cavity resonance method, and 4) requirement of high Q for the separation of CW and CCW modes upon rotation of the cavity.

Beside these, the future evolution of the present work is to resolve the two challenges: namely 1) the rotational effect of the proposed cavity and 2) the improvement of total reflection ability for an accurate measurement of rotational speeds.

5. CONCLUSION

The proposed cavity resonator is yet another application of self-collimation effect in photonic crystal. The characterization study establishes the confinement, field enhancement and energy storage ability of the proposed cavity. The wave-confinement effect is mainly attributed from divergence-less beam propagation and it is the main difference of the photonic crystal cavity over the conventional ones. The cavity lifetime calculations verify the confinement effect with the presence of dielectric losses in the system. This is one of the advantages over the negative refraction based cavity resonators formed by PCs, where the wave-confinement in negative refraction based cavity is no longer maintained upon the inclusion of dielectric losses. The estimated Q factor value of the proposed cavity is of the order of 10^3–10^4. The analysis also reveals that the horizontal position of the line source plays an effective role on the maximum limit of the quality factor. The field inside the cavity resonator is studied through finite-difference time-domain methodology for a short Gaussian pulse placed inside the cavity and the minimum radiation losses reveal the energy storage

aspect. Owing to the divergence less beam propagation due to the self-collimation effect and the confinement with minimum radiation losses, the proposed cavity resonator can be used as Sagnac ring for gyroscopes applications in microwave/optical regime, though there are some challenges need to be taken up to improve the reflection and rotational effect of the cavity.

REFERENCES

1. Yablonovitch, E., "Inhibited spontaneous emission in solid-state physics and electronics," *Phys. Rev. Lett.*, Vol. 58, No. 20, 2059–2062, 1987.
2. Kosaka, H., T. Kawashima, A. Tomita, M. Notomi, T. Tamamura, T. Sato, and S. Kawakami, "Self-collimating phenomena in photonic crystals," *Appl. Phys. Lett.,* Vol. 74, No. 9, 1212–1214, 1999.
3. Luo, C., S. G. Johnson, J. D. Joannopoulos, and J. B. Pendry, "All-angle negative refraction without negative effective index," *Phys. Rev. B*, Vol. 65, 201104(R), 2002.
4. Yu, X. and S. Fan, "Bends and splitters for self-collimated beams in photonic crystals," *Appl. Phys. Lett.,* Vol. 83, No. 16, 3251–3253, 2003.
5. Zabelin, V., L. A. Dunbar, N. L. Thomas, R. Houdré M. V. Kotlyar, L. O'Faolain, and T. F. Krauss, "Self-collimating photonic crystal polarization beam splitter," *Opt. Lett.*, Vol. 32, No. 5, 530–532, 2007.
6. Luo, C., S. G. Johnson, J. D. Joannopoulos, and J. B. Pendry, "Subwavelength imaging in photonic crystals," *Phys. Rev. B*, Vol. 68, 045115, 2003.
7. Ruan, Z. and S. He, "Open cavity formed by a photonic crystal with negative effective index of refraction," *Opt. Lett.,* Vol. 30, No. 17, 2308–2310, 2005.
8. Ramakrishna, S. A., S. Guenneau, S. Enoch, G. Tayeb, and B. Gralak, "Confining light with negative refraction in checkerboard metamaterials and photonic crystals," *Phys. Rev. A*, Vol. 75, 063830, 2007.
9. Tanaka, Y., J. Upham, T. Nagashima, T. Sugiya, T. Asano, and S. Noda, "Dynamic control of the Q factor in a photonic crystal nanocavity," *Nature Mater.*, Vol. 6, 862–865, 2007.
10. Shen, X.-P., H. Kui, Y. Fang, H.-P. Li, Z.-Y. Wang, and Q. Zhong, "New configuration of ring resonator in photonic crystal based on

self-collimation," *Chinese Physics Letters*, Vol. 25, No. 12, 4288–4291, 2008.

11. Whiteman, J. R., *The Mathematics of Finite Elements and Applications*, John Wiley and Sons, Chichester, 1998. http://www.comsol.com.
12. Taflove, A. and S. C. Hagness, *Computational Electrodynamics — The Finite-difference Time-domain Method*, Artech House, Boston, 2000.
13. Johnson, S. G. and J. D. Joannopoulos, "Block-iterative frequency-domain methods for Maxwell's equations in a plane wave basis," *Opt. Express*, Vol. 8, No. 3, 173–190, 2001. http://ab-initio.mit.edu/mpb.
14. Foteinopoulou, S. and C. M. Soukoulis, "Electromagnetic wave propagation in two-dimensional photonic crystals: A study of anomalous refractive effects," *Phys. Rev. B*, Vol. 72, 165112, 2005.
15. Nagesh, E. D. V., N. Yogesh, and V. Subramanian, "Application of defect induced microwave band gap structure for non-destructive evaluation and the construction of a frequency selector switch," *PIERS Online*, Vol. 4, No. 6, 631–634, 2008.
16. Oskooi, A. F., D. Roundy, M. Ibanescu, P. Bermel, J. D. Joannopoulos, and S. G. Johnson, "MEEP: A flexible free-software package for electromagnetic simulations by the FDTD method," *Comp. Phys. Commun.*, Vol. 181, 687–702, 2010.
17. Post, E. J., "Sagnac effect," *Rev. Mod. Phys.,* Vol. 39, No. 2, 475–493, 1967.
18. Sunada, S. and T. Harayama, "Sagnac effect in resonant microcavities," *Phys. Rev. A*, Vol. 74, 021801(R), 2006.
19. Steinberg, B. Z. and A. Boag, "Splitting of microcavity degenerate modes in rotating photonic crystals-the miniature optical gyroscopes," *J. Opt. Soc. Am. B*, Vol. 24, No. 1, 142–151, 2007.